THE ROYAL SOCIETY

Computational analysis of functional connectivity between areas of primate cerebral cortex

Klaas E. Stephan[1], Claus-C. Hilgetag[2], Gully A. P. C. Burns[3], Marc A. O'Neill[2], Malcolm P. Young[2] and Rolf Kötter[1,4*]

[1]*C. & O. Vogt Brain Research Institute, and* [4]*Institute of Morphological Endocrinology and Histochemistry, Heinrich Heine University, D-40225 Düsseldorf, Germany*

[2]*Neural Systems Group, Department of Psychology, University of Newcastle upon Tyne, Ridley Building, Newcastle upon Tyne NE1 7RU, UK*

[3]*Department of Neurobiology, University of Southern California, Los Angeles, CA 90089-2520, USA*

Recent analyses of association fibre networks in the primate cerebral cortex have revealed a small number of densely intra-connected and hierarchically organized structural systems. Corresponding analyses of data on functional connectivity are required to establish the significance of these structural systems. We therefore built up a relational database by systematically collating published data on the spread of activity after strychnine-induced disinhibition in the macaque cerebral cortex *in vivo*. After mapping these data to two different parcellation schemes, we used three independent methods of analysis which demonstrate that the cortical network of functional interactions is not homogeneous, but shows a clear segregation into functional assemblies of mutually interacting areas. The assemblies suggest a principal division of the cortex into visual, somatomotor and orbito-temporo-insular systems, while motor and somatosensory areas are inseparably interrelated. These results are largely compatible with corresponding analyses of structural data of mammalian cerebral cortex, and deliver the first functional evidence for 'small-world' architecture of primate cerebral cortex.

Keywords: primate cerebral cortex; strychnine neuronography; epilepsy; optimization analysis; graph theory; multidimensional scaling

1. INTRODUCTION

As the amount of information on the cerebral cortex is rapidly growing, analyses of this information become indispensable for unravelling its complex structural and functional organization. In recent years, a variety of analytical methods have been successfully applied to data on association fibres revealed by anterograde and retrograde tracing studies in the cerebral cortex of mammals. For example, hierarchical analysis of laminar patterns of fibre terminations classified as ascending, descending or lateral showed that the primate visual system is hierarchically organized (Felleman & Van Essen 1991), but that it is nonetheless not possible to determine a unique visual hierarchy from this information (Hilgetag *et al.* 1996). Optimization analysis of the topological organization of cortical areas in cats and primates demonstrated that all major sensory systems are organized sequentially, that some sensory systems are divided structurally into 'streams of processing', that the cortical motor system is embedded in the somatosensory system, and that the prefrontal and mesial areas are connectionally associated with each other and with the least peripheral sensory-processing regions (e.g. Scannell *et al.* 1995; Young 1992, 1993; Young *et al.* 1994).

The significance of these structural analyses will be determined by the extent to which insights into the structural organization of the cerebral cortex can help to unravel the principles of cortical function. If association fibre connectivity correlates with the propagation of activity in the cerebral cortex, then it might be possible to predict the patterns and spread of activity from data on anatomical connectivity, or to infer the influence of association fibre connectivity from functional imaging paradigms. However, the detailed investigation of activity propagation in the primate cerebral cortex *in vivo* is hampered by major technological and ethical problems. At the gross level required for the delineation of major functional systems, however, relevant data have already been available for many decades. It is seldom remembered now that, in the 1930s to 1950s, large parts of the cerebral cortex of the macaque were systematically tested *in vivo* for the propagation of locally induced epileptiform activity by strychnine neuronography. To date, the large quantities of this information on activity spread have not been analysed systematically (see Kötter & Sommer (this issue) and Sommer & Kötter (1997) for a preliminary analysis). We were interested in whether the application of modern computational analysis tools could reveal evidence for

*Author for correspondence (rk@hirn.uni-duesseldorf.de).

functionally defined cortical systems, and whether such systems would be organized in a way that is consistent with the anatomical systems recently demonstrated in the cerebral cortex of the macaque monkey (e.g. Young 1993; Young *et al*. 1994). A preliminary report of this work has appeared in abstract form (Hilgetag *et al*. 1997).

2. METHODS

(a) *Data*

We collated data from 19 published strychnine neuronographic studies, including a total of 3897 tests for propagation of epileptiform activity in all cortical regions of the macaque cortex after 245 different local cortical applications of strychnine *in vivo* (Bailey *et al*. 1943*a*,*b*, 1944*a*,*b*; Chusid *et al*. 1948; Dunsmore & Lennox 1950; Dusser de Barenne & McCulloch 1938; Dusser de Barenne *et al*. 1938, 1941; French *et al*. 1948; Petr *et al*. 1949; Pribram *et al*. 1950; Pribram & MacLean 1953; Sugar *et al*. 1948, 1950*a*,*b*,*c*; Von Bonin *et al*. 1942; Ward *et al*. 1946). All studies employed the method of strychnine neuronography as initially developed by Dusser de Barenne (see Dusser de Barenne 1924 and Dusser de Barenne & McCulloch 1938, 1939 for detailed discussions of the methodology) and were performed according to very similar experimental protocols. The general principle of strychnine neuronography is the following: application of strychnine to the cortical surface leads to local disinhibition by the antagonistic effects of strychnine on cortical $GABA_A$ and glycine receptors (Klee *et al*. 1992; Shirasaki *et al*. 1991; Takahashi *et al*. 1994). The activity is first observed locally and then spreads to spatially remote cortical sites. According to Dusser de Barenne & McCulloch (1938), the evolving global pattern of activity reaches a steady state after 2–3 min and remains stable for up to 15 min after removal of the stimulus. They emphasized that the strychnine-induced activity patterns are reproducible within the same animal and stable for any given area across animals. Exploring the functional organization of sensory cortex, Dusser de Barenne & McCulloch (1938) also found that the patterns of activity due to strychnine neuronography matched those elicited by electrical stimulation. Since neither deep undercutting of the cortex nor circular thermocoagulation throughout the entire thickness of the cortex around strychninized cortical sites changed strychnine-induced activity patterns, they concluded that the activity elicited by strychnine was conveyed by corticocortical association fibres. Until the mid-1950s, strychnine neuronography was extensively used for the detection of association pathways. However, it could not be clarified experimentally whether the propagation of strychnine-induced activity was restricted to monosynaptic connections or also occurred across synapses (Dusser de Barenne & McCulloch 1939; Frankenhaeuser 1951). Recent computer simulations of strychnine-induced epileptiform activity spread in cat cerebral cortex (Kötter & Sommer, this issue) clearly showed that assuming monosynaptic propagation accounts poorly for the observed patterns of activity, whereas polysynaptic propagation reproduced these patterns significantly better. It therefore seems very likely that the neuronographic data rather reflect polysynaptic than monosynaptic propagation of activity.

The global cortical steady states of propagated activity after local strychnine application represent stable and reproducible temporal correlations between spatially remote neurophysiological events. Applying the definition of Friston (1994), they specify the functional connectivity between a disinhibited (strychninized) cortical area A and all other areas B_i ($1 \leqslant i \leqslant$ number of all cortical areas). For each pair (A, B_i), the interaction can be positive (activity propagates from area A to area B_i), negative (area B_i was investigated, but no activity spread from A was found), or it may be unknown (area B_i was not investigated).

We stored and processed the data by means of a specifically designed relational database (CoCoMac-Stry) implemented with Microsoft Access (v. 7.0, Windows 95). This system maintains the original nomenclature of the experimental findings and provides coordinate-independent algorithms for optimal data conversion into freely chosen cortical parcellation schemes by using objective relational transformation (ORT—see the companion paper of Stephan *et al*. (this issue) for a detailed description). In the present study, the experimental findings of the various experiments were mapped by ORT to three parcellation schemes (McCulloch 1944; Von Bonin & Bailey 1947; Walker 1940). Since the accuracy of these maps varied for different regions of the cortex, we present the results of the analyses in a 'hybrid map' (figure 1). Von Bonin & Bailey's (1947) map for the macaque cortex, which is well known but of low precision for the prefrontal cortex, was merged with Walker's (1940) parcellation of the prefrontal cortex, which is still widely used. The combination of these two parcellation schemes provided a balance between optimal precision of localization and experimental limitations, and forms the basis for many modern parcellation schemes (e.g. Barbas & Pandya 1989; Carmichael & Price 1994; Felleman & Van Essen 1991; Pandya & Seltzer 1982; Preuss & Goldman-Rakic 1991). As a control, the data mapped to the scheme of McCulloch were analysed in exactly the same way as the data mapped to the hybrid map. Whereas in this paper we only present the results in the hybrid map, the companion paper of Stephan et *al*. (this issue) includes a comparison of some results in both maps.

For the analyses, the data were classified in two ways. Binary classification differentiated positive and absent activity spread, whereas weighted classification distinguished five categories of activity spread: absent (0), weak (1), moderate (2), strong (3) and positive activity spread of unknown strength (X) (figure 2). Our intention was to find out whether the mere existence or absence of functional interactions alone would determine the outcome of the analysis, or whether the strengths of the individual interactions played an important role. Also, the binary data served as a control for potential biases within the weighted data due to methodological restrictions of strychnine neuronography (see § 4). Both classifications distinguished between interactions explicitly reported absent and those hitherto unstudied by neuronographic methods. The cortical network represented by these data was analysed for topological properties and functional clusters by three independent methods, which are described in the following sections.

(b) *Graph-theoretical 'small-world' analysis*

As a first statistical method, we used a graph-theoretical approach, which has been introduced recently for the structural investigation of networks (Watts & Strogatz 1998). This method assesses the global structural properties of a given network by reference to two values. The characteristic path length, L, indicates the average shortest separation of any two nodes of the network (i.e. the number of sequential connections that are necessary, on average, to link one area to another by the shortest pathway), whereas the clustering coefficient, C, characterizes the 'cliquishness' of the network (i.e. the tendency of the network to form local clusters of densely connected areas). Computing these values for 20 random matrices of the same size, density and proportions of existing to absent interactions as our real network

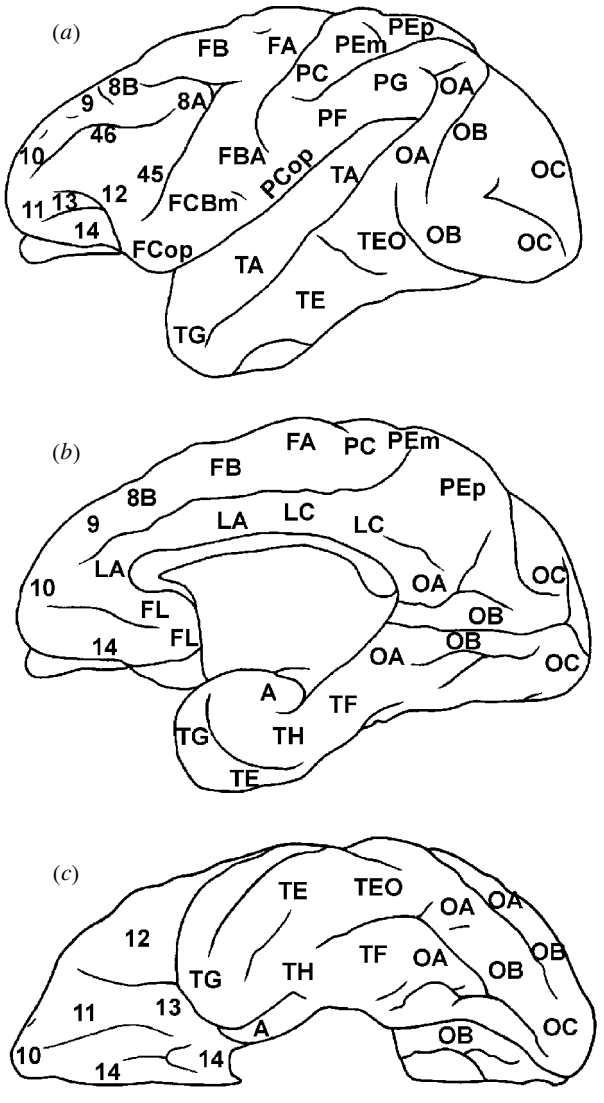

Figure 1. Schematic map of the hybrid parcellation scheme in which the results of this study are presented. Labels designate approximate positions of areas. Prefrontal areas are named according to Walker (1940), all other areas according to Von Bonin & Bailey (1947). Sulcal morphology is adopted from Preuss & Goldman-Rakic (1991*a*,*b*). Insular areas IA and IB, supratemporal areas TB and TC, and postcentral area PB are concealed by the lateral fissure and the central sulcus, respectively. (*a*) Lateral aspect. Note that this view also shows parts of the orbital cortex, i.e. areas 11, 13 and 14; (*b*) medial aspect; (*c*) ventral aspect.

allowed us to compare the properties of the actual network of interactions with the normal features of randomly connected networks. We used a program implemented with Visual Basic and Microsoft Excel 7.0 (Windows 95) to compute these values according to the definitions by Watts & Strogatz (1998).

(c) *Optimal set analysis*

Next, we applied an evolutionary optimization approach, called optimal set analysis (OSA), originally developed for analysis of anatomical connectivity (see Hilgetag, Burns, O'Neill, Scannell & Young, this issue). This approach focuses on the cerebral cortex as a network of interconnected areas and evaluates the identities of clusters of strongly related structures by minimizing explicit cost functions. The central idea is that optimal sets of areas are characterized by a maximum of intra-set connection density and a minimum of inter-set connectivity (see Tononi *et al.* (1998) for a similar approach). Accordingly, a two-component cost function is defined consisting of an 'attraction' cost (C1: the number of actual relationships between different sets), and a 'repulsion' cost (C2: the number of possible, but absent relationships within sets of areas). The analysis begins by the creation of random sets of areas, whose intra-set and inter-set connection densities are then calculated. In an iterative process of mutation and selection, individual areas are taken out of one set and attributed to another set of areas, the costs of these new arrangements evaluated and lower-cost solutions evolved further until the total cost is minimal. Details of this approach are described elsewhere (Hilgetag *et al.* 1998; Hilgetag, Burns, O'Neill, Scannell & Young, this issue).

The strength of the individual interactions entering the attraction component of the cost function depended on the data classification. For data in the binary classification (existing and absent interactions), there was only one attraction strength (set to the numerical value of 1). For the weighted data originally classified in five different categories (see above), there were three different levels for the strength of existing interactions: weak activation or activation of unknown strength (numerical value of 1), moderate activation (2) and strong activation (3). Unstudied interactions were excluded from the analyses.

By varying the relative weights of attraction and repulsion in the combined cost function, we created series of cluster arrangements differing in the number and composition of the optimal clusters. Weights in the series ranged from a maximal attraction weight of 11 to a maximal repulsion weight of 7. Throughout the series, we varied either attraction or repulsion by steps of 1 while keeping the other constant at 1. The different constellations of attraction and repulsion weightings emphasized specific aspects of the resulting area groupings. The most important parameter constellations of OSA were as follows.

(i) Balance: attraction and repulsion were of equal value (set to 1), that is, existent interactions between the clusters and absent interactions within the clusters contributed equally to the cost of the cluster structure. Clusters computed with this option tended to be of intermediate size.

(ii) High attraction: attraction was as large as necessary to ensure that clusters could not be further amalgamated. This constellation demonstrated independent functional units by leaving unmerged only those clusters that were completely disconnected.

(iii) High repulsion: repulsion was as large as necessary to remove all absent interactions from within the clusters, and thereby locate them outside the resulting clusters. Clusters could thus be envisaged as a maximally dense functional core within a network of communicating areas. We have previously named these clusters 'building blocks' (Hilgetag *et al.* 1998), as they could not be subdivided any further by increasing the repulsion weight.

(iv) Average: series of cluster arrangements were computed between high repulsion and high attraction as described above. Averaging across these results emphasized features of the cluster configurations that were constant irrespective of the detailed parameters of the cost functions. Due to the blurring effect of averaging, however, the resulting clusters showed less sharp borders and more complicated structure.

In repeated optimization series, every candidate cluster arrangement that possessed a cost lower than, or within a 1% band of,

the lowest cost of all other cluster configurations, and which was different from all other previous solutions was stored. The resulting population of optimal solutions was summarized by 'cluster plots' of the cortical areas (e.g. figures 3*a*,*b*, 4*b* and 5*a*). These plots are symmetrical matrices in which each entry reflects the frequency with which the respective pair of areas was found within a common cluster across all optimal cluster configurations (see Hilgetag, Burns, O'Neill, Scannell & Young (this issue) for details). We called this relative number the 'association' between the two cortical areas. For any given area, the vector of its association with all other areas (i.e. its row or column in the cluster plot) was called the 'association vector.'

(d) *Statistical evaluation of optimal set analysis results*

Generally, we evaluated the resulting OSA cluster plots according to two principles.

(i) As a general 'cluster threshold', we considered two areas to be within the same cluster if they were grouped together in more than half of all optimal solutions, that is, if their mutual association was at least 50%.

(ii) We applied a 'bridging principle' for cluster membership. Two areas A and C were considered to belong to the same cluster, if there were areas B_1 to B_n ($n \geqslant 1$), for which each of the associations (A, B_1), (B_1, B_2), ..., (B_{n-1}, B_n), (B_n, C) were higher than the chosen cluster threshold.

To show the specificity of our OSA results we used two statistical methods that compared the results of the analyses of the original data with results obtained from randomized data. The matrices of randomized data were derived from the original data matrices by random reshuffling of the entries to keep the number and proportion of positive and absent interactions constant. Twenty matrices of random binary data were created both for the hybrid map and the map of McCulloch (McCulloch 1944). These random matrices were then processed by OSA (balanced condition) in exactly the same way as the real data. First, to determine the degree of agreement between the OSA results for random and real data, we computed the linear correlation coefficient between the OSA result for each random data matrix and the real data matrix. For this purpose, we applied the Correl function of the Analysis Toolpack in Microsoft Excel 7.0 (Windows 95) to corresponding matrix fields of the respective cluster plots. As a second method, we determined the distribution of lowest costs across all random matrices and compared this to the lowest cost of the original data set.

Furthermore, we investigated whether the classification of the data had any influence on the results by performing the analyses both for the weighted and the binary data. The results were then compared by a correlation analysis as described above.

Finally, we used hierarchical cluster trees for an alternative representation of cluster configurations of OSA results by applying the Hierarchical Clustering method of SYSTAT 8.0 (SPSS, Inc.) to the OSA results, using an Euclidean distance metric and single linkage (see figures 4*a* and 5*b*). We restricted this representation to areas from the three main clusters that constantly emerged from all analyses (compare figure 7). Hierarchical cluster trees demonstrate the structure of cluster sets by revealing hierarchical degrees of similarity between the clusters. Starting with single areas on the left, repeated amalgamation of areas (or resulting clusters) occurs at the Euclidean distance between the association vectors of the two areas (or of the two closest members of the clusters, respectively). Vice versa, one may imagine the reverse process as one initial big cluster on the right that is repeatedly split: the sooner a cluster splits, the less similar are the resulting subclusters. The process of splitting is continued until areas are either isolated or indistinguishable (i.e. their association vectors have a Euclidean distance of zero). Representation of OSA results by cluster trees is especially useful for a comparison of high repulsion and averaged OSA (see legends of figures 4*a* and 5*b*).

(e) *Non-metric multidimensional scaling*

We employed non-metric multidimensional scaling (NMDS) as a third, independent method to investigate the organization of functional interactions among cortical areas. We here briefly summarize the main principles of this method as its application to neuroanatomical data has already been described in detail (Burns 1997; Burns & Young, this issue; Young *et al.* 1995). NMDS provides high-dimensional metric representations of a given set of elements with non-metric relationships (like anatomical connectivity or functional interactions between cortical areas), so that the distances between the elements in the high-dimensional space optimally represent the non-metric constraints. In the context of our analysis, NMDS tends to group together areas that are strongly interacting and tends to separate objects without interactions. For ease of visualization, we have constrained these spatial representations to two dimensions.

Calculations on the untransformed matrices of interactions were performed using the MDS procedure in the SAS statistical software package (v. 6.11 for Windows; SAS Technical Report P-229 SAS/STAT Software: changes and enhancements. Chapter 15: the MDS procedure). We generated two-dimensional NMDS configurations using cost functions with FIT = 0.5, 1 and 2 under the tied and untied approaches in the SAS/STAT MDS procedure (see Burns & Young, this issue).

3. RESULTS

(a) *Statistics of functional connectivity data*

For the 39 areas of our hybrid map, the experimentally determined matrix contained 649 reports on positive and absent spread of activity: that is, information about 43.8% of all possible interactions (figure 2). 34.1% of the available information reported spread of activity to cortical areas other than the strychninized one, and the remainder showed absence of activity spread. Information on individual areas showed a considerable variance: on average, 42.9% of all possible interactions were examined for an individual area with a standard deviation of 17.1%. The range between the area studied most (premotor area FB 69.7%) and least intensively (prefrontal area 12 10.5%) approximated a factor of seven. For prefrontal areas 8A, 8B, 9, and 12 only absence of activity spread was reported. These differences of data background are important for the interpretation of the analytical results. Finally, it should be noted that no data were available for prefrontal area 14 (see figure 2). Therefore, this area had to be excluded from the analyses.

(b) *Graph-theoretical 'small-world' analysis*

The values L (characteristic path length) and C (clustering coefficient) for the real network were $L_{\text{real}} = 2.1730$ and $C_{\text{real}} = 0.3830$. The statistical distribution of these values for 20 random networks of the same size and

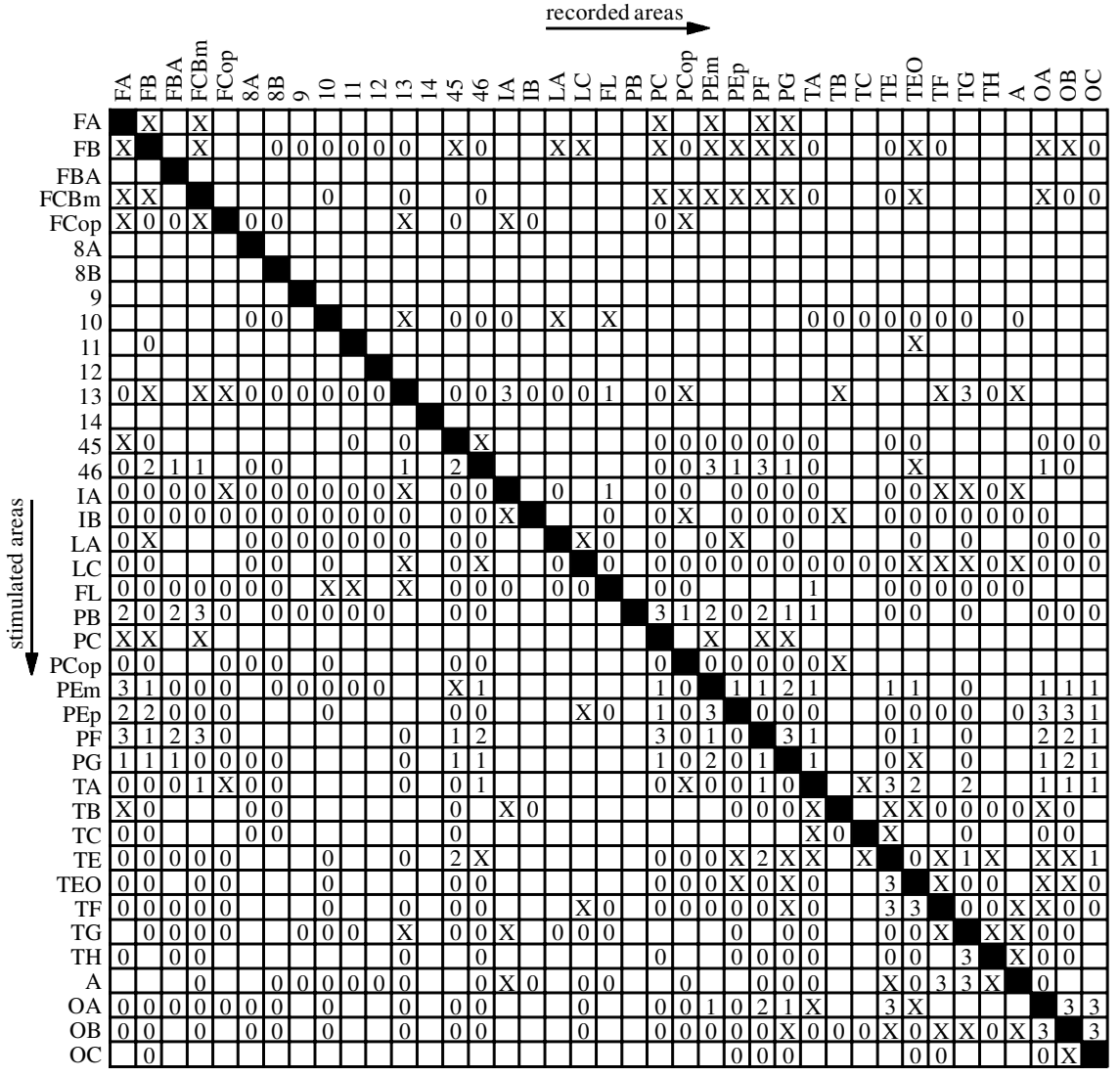

Figure 2. Matrix of functional connectivity in macaque cortex. Spread of activity between cortical areas of the macaque as determined by strychnine neuronography. Areas strychninized are listed in rows and recorded areas in columns. Properties of propagated activity are indicated in the following way: 0, absent; 1, weak; 2, moderate; 3, strong; X, activity spread of unknown strength; blank fields, not investigated. Areas are named according to a combined scheme of Von Bonin & Bailey (1947) and Walker (1940); see figure 1.

density delivered the following values: L_{rnd}, mean = 2.1500, s.d. = 0.0164; C_{rnd}, mean = 0.1557, s.d. = 0.0149.

The characteristic path length L_{real} of our real network is not significantly higher than the mean path length between nodes of a random network (L_{real} is less than 1.5 standard deviations apart from the average L_{rnd}), whereas the clustering coefficient C of our real network is significantly larger than could be expected for any random network (C_{real} is more than 15 standard deviations higher than C_{rnd}). This constellation ($L_{real} \approx L_{rnd}$ but $C_{real} \gg C_{rnd}$) is consistent with the definition of a 'small-world' network (Watts & Strogatz 1998), that is our real network maintains a highly clustered structure while still assuring that any two of its members are not significantly further apart than they would be in a randomly connected network. As randomly connected networks on average possess very low characteristic path lengths, this feature indicates that interactions in the actual network are very efficiently distributed. The position of C_{real} within the distribution for C_{rnd} makes it extremely unlikely that the clustered structure of our real network could be mimicked by a randomly constructed network of the same size and connection density.

If our data on functional connectivity characterize a very efficiently structured network (highly clustered structure plus low communication costs), what areas constitute these clusters, and what might be their functional context? These questions were addressed by applying OSA and NMDS to the data.

(c) *Optimal set analysis*

This section describes the OSA results, comparing the three-parameter constellations—balanced, high repulsion and averaged—between the binary and weighted classification of the data in detail (see figure 7 for a summary). As for high attraction, this condition led, for both binary and weighted data, to the formation of one large cluster comprising all but the four poorly investigated prefrontal areas with no reported interactions (see above). This result demonstrates that the functional cortical network

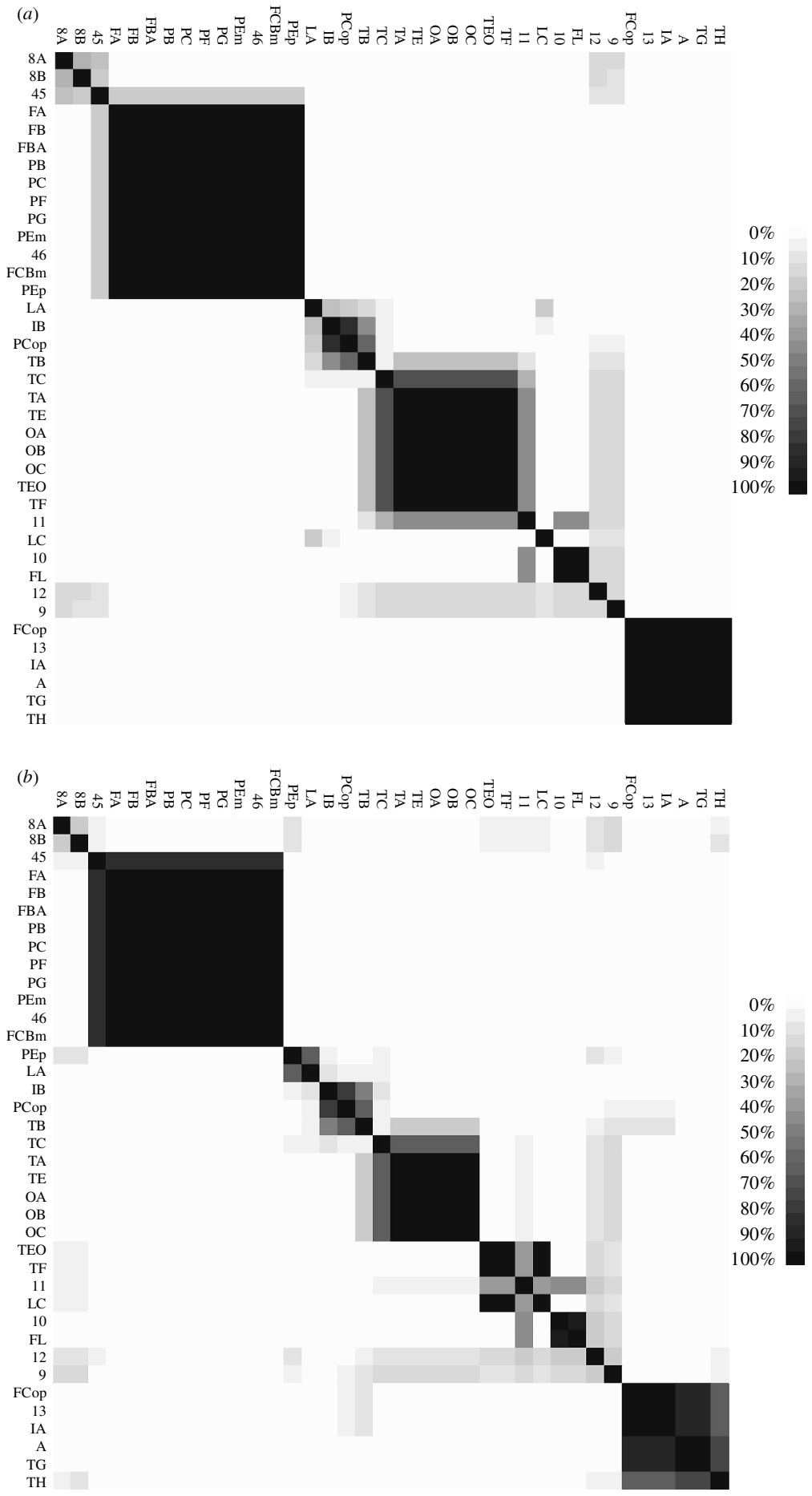

Figure 3. Cluster plots of results from balanced OSA, both for the (*a*) weighted data and (*b*) the binary data. Matrices have been ordered identically to allow a direct comparison (note the high similarity between the results) and to optimally reflect the cluster configuration of both results. Intensity of shading indicates how frequently two areas were found to share the same cluster across all optimal groupings. Areas are named according to the hybrid map of figure 1.

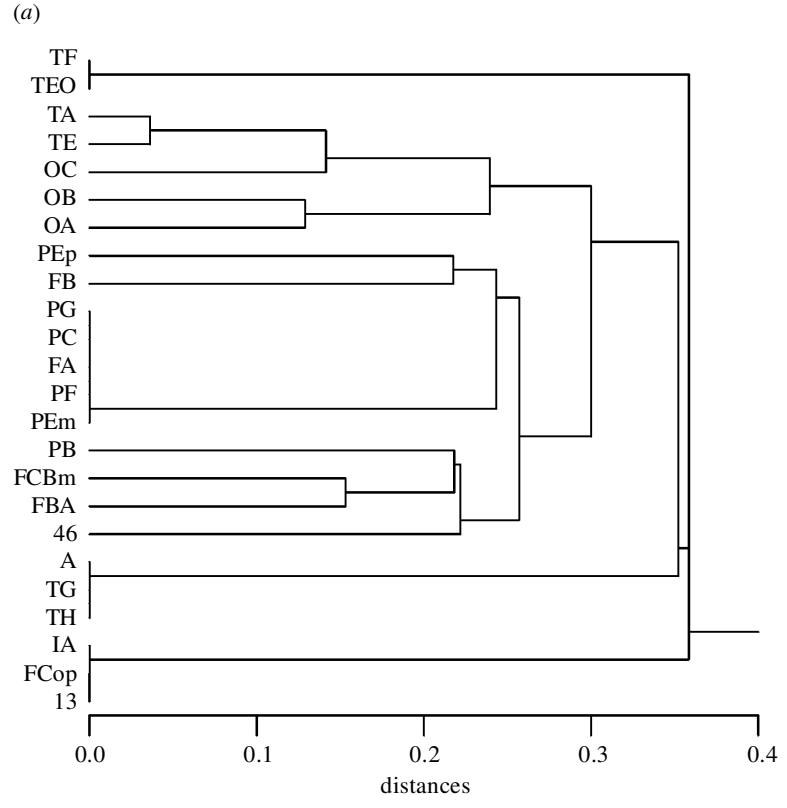

Figure 4. (*a*) Hierarchical cluster tree of the three main clusters resulting from high-repulsion OSA in case of the weighted data. Comparing this representation to the cluster tree of averaged OSA (figure 5*b*) illustrates the differences between these OSA parameter constellations. High repulsion as in this figure favours rather small, clearly defined, dissimilar clusters, thus splitting occurs at comparatively high distances (see § 2). (*b*) Cluster plot of high repulsion OSA for the binary data. Nomenclature and shading as in figure 3.

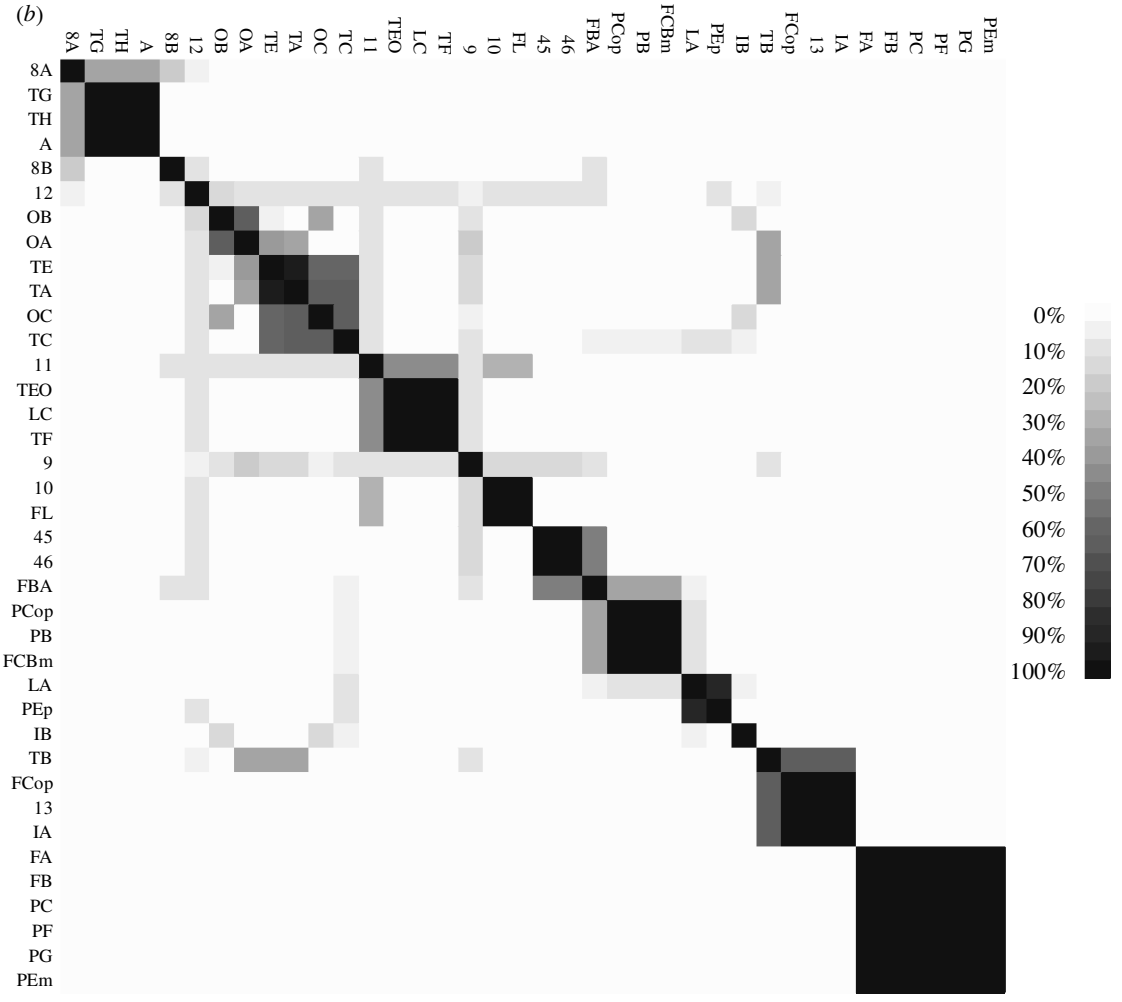

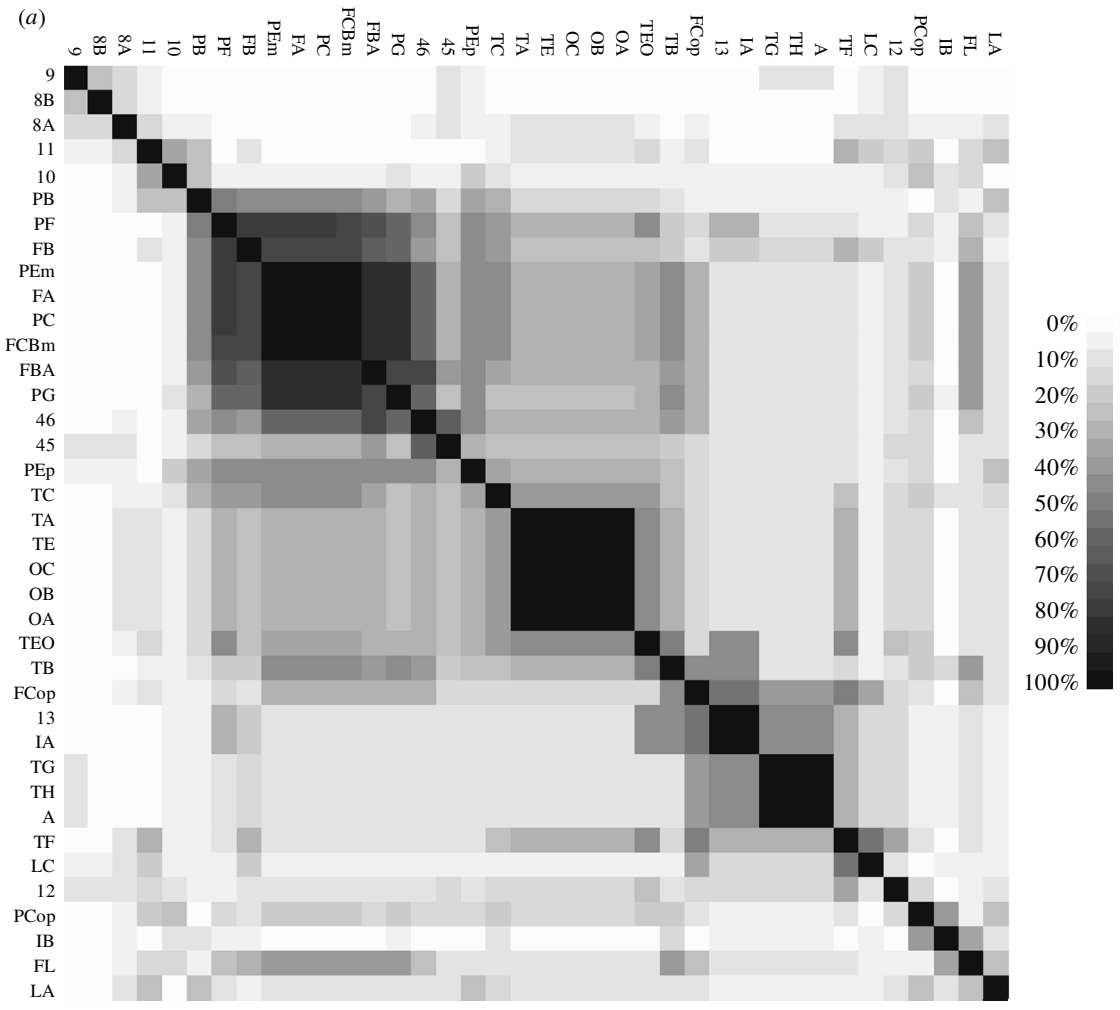

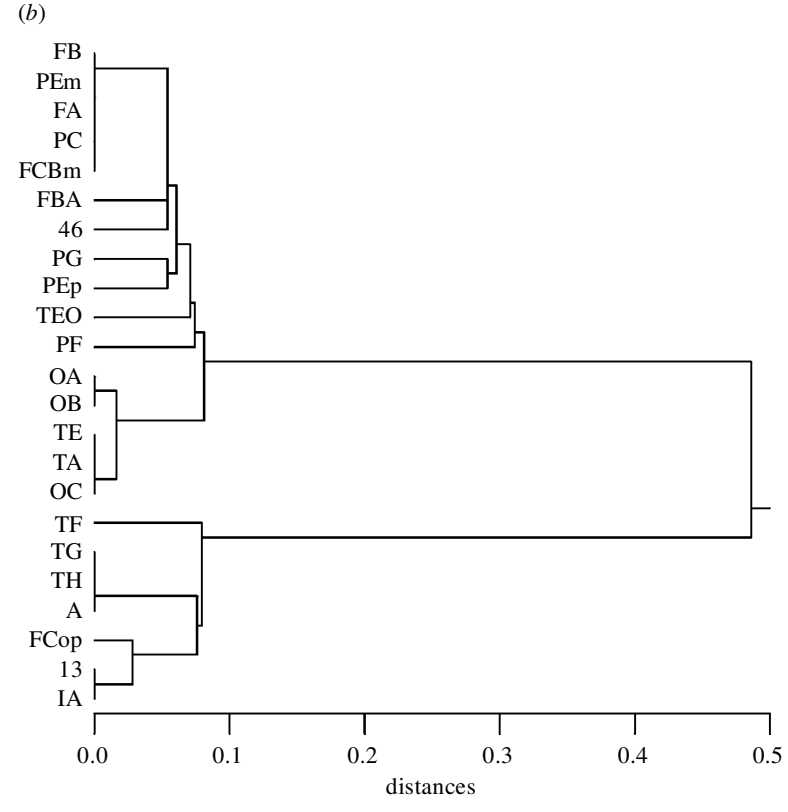

Figure 5. (*a*) Cluster plot of averaged OSA for the weighted data. Nomenclature and shading as in figure 3. (*b*) Hierarchical cluster tree of the three main clusters from averaged OSA results in case of the binary data. A comparison with figure 4*a* clearly shows the differences between high repulsion and averaged OSA: for the averaged condition shown in this figure, there is a tendency towards large clusters with fuzzier borders, reflected by the rather low distances at which final clusters separate in this figure (see §2). In this case, this is especially obvious for the somatomotor and the visual cluster.

does not contain clusters completely devoid of influences from other clusters.

In the following, we indicate the range from the lowest to the highest association if we describe several areas of the same cluster but with different degrees of association. Starting with the balanced condition, OSA delivered three main clusters for the weighted data (figure 3*a*).

(i) A first cluster comprised the primary motor area (area FA), the lateral and medial premotor areas (areas FB, FBA, FCBm), the primary sensory cortex (areas PB, PC) and parietal areas (areas PEm, PEp, PF, PG), as well as lateral prefrontal area 46. All areas of this cluster had a mutual association of 99.2–100%. We refer to this cluster as the somatomotor cluster.

(ii) A second cluster contained the primary visual cortex (area OC), extrastriate visual cortex (areas OA, OB), temporo-occipital cortex (area TEO), superior temporal cortex including parts of the superior temporal sulcus (area TA), inferotemporal cortex (area TE) and medial temporal cortex (area TF). All areas had a mutual association of 100%. We called this cluster the visual cluster. In 69.2% of all optimal solutions the primary auditory cortex (area TC) also fell into this group. This is due to the rather limited amount of data available for this area (for area TC only 19.7% of all possible interactions were investigated, only four of which showed spread of activation; these were reciprocal interactions with temporal areas TA and TE (see figures 2 and 6*a*,*b*)).

(iii) A third cluster contained areas of orbitofrontal cortex and the frontal operculum (areas 13 and FCop), anterior insular cortex (area IA) and polar, medial and allocortical regions of the temporal lobe (areas TG, TH and A, respectively). Again, the association between the areas of this cluster was 100%. We refer to this group as the orbito-temporo-insular cluster.

Two further small clusters were observed in this case but were not consistently reproduced under other conditions. The first consisted of two prefrontal areas, namely frontopolar area 10 and medial subcallosal area FL, which were associated by 100%. The second contained posterior insula cortex (area IB), parts of the supratemporal plane (area TB) and the parietal operculum (area PCop). The association between these areas ranged between 61.7 and 83.1%. Eight areas did not cluster but remained isolated: prefrontal areas 8A, 8B, 9, 11, 12, 45 and cingulate areas LA and LC. Except for area 45, the isolated position of these prefrontal areas was due to the small amount of data available about their interactions (between 10.5–26.3% of all possible interactions were examined, all of which were absent for areas 8A, 8B, 9, 12; figure 2).

The results of balanced OSA for the binary data (figure 3*b*) and weighted data yielded very similar results as established by a correlation analysis ($r = 0.82$, see below). The most notable difference was that the visual areas TF and TEO did not cluster with the other visual areas but formed a group on their own, joined by posterior cingulate area LC (association 97.8–100%). Also, the orbito-temporo-insular cluster, which comprised the same areas as seen with the weighted data, showed a subtle splitting: the orbitofrontal and insular areas (areas 12, FCop and IA), on the one hand, and the temporal areas (areas TG and A), on the other hand, each showed a cluster association of 100%, while these two groups still clustered in 90.2% of the optimal solutions. The associations of area TH with the other areas of this cluster were weaker than in the case of the weighted data (67.4–77.2%). Finally, two minor differences of the somatomotor cluster were noticed: compared to the weighted data, superior parietal area PEp clustered more strongly with anterior cingulate area LA (association of 66.8%) than with the other areas of the somatomotor cluster; lateral prefrontal area 45 which remained isolated in the case of the weighted data, joined the somatomotor cluster (association of 84.2%).

High repulsion split the clusters obtained by the balanced condition into smaller clusters with no remaining absent interactions between their members, the so-called 'building blocks'. This splitting into subclusters is visualized especially well by the hierarchical cluster tree shown for weighted data in figure 4*a*. The results for binary and weighted data were again highly similar (the correlation between the cluster plots was $r = 0.93$, see below).

For both data classifications, the orbito-temporo-insular cluster split into an orbito-insular (areas 13, FCop, IA) and a temporal (areas TG, TH, A) subcluster, each having cluster associations of 100%. The visual cluster showed a similar splitting into three visual subgroups: the primary visual cortex OC clustered loosely (weighted data: 61.2–64.7%; binary data: 60.0–64.0%) with the strongly associated superior and inferior temporal areas TA and TE (weighted data: 94.1%; binary data: 96.0%). Areas TF and TEO (both cases: 100%) formed a second subgroup, and areas OA and OB (weighted data: 65.9%; binary data: 64.0%) a third. In contrast to the orbito-temporo-insular and visual clusters, the somatomotor cluster showed a less distinct subdivision. The majority of its members remained closely associated, especially primary motor area FA, premotor area FB, primary sensory area PC and lateral parietal areas PEm, PF and PG all of which maintained an association of 100% in case of the binary data and of 98.8–100% for the weighted data (in the latter case, area FB was less strongly associated with 51.8–52.9%).

Finally, we looked at the results of the average condition for both weighted and binary data (figure 5*a*,*b*). Again, the results for binary and weighted data were very similar, the correlation between the respective cluster plots being $r = 0.83$ (see below). Because of the 'summarized' features of cluster configuration with fuzzier, less clear-cut clusters, the three main clusters are somewhat less separable than for the other conditions. This is especially obvious for the binary data where the visual and somatomotor cluster show a tendency to merge (note the low distance at which the two clusters separate in the clustertree of figure 5*b*). As for the somatomotor cluster, the most cohesive areas across all parameter constellations were primary motor area FA, primary sensory area PC, premotor areas FB and FCBm, and parietal area PEm. These areas showed mutual associations of 96.4–100% for the binary data and 99.1–100% for the weighted data (for the latter, FB was less strongly connected with 74.7–75.2%). To this core, all other areas

of the somatomotor cluster remained closely associated. Only prefrontal area 46 (weighted data 32.7–73.3%; binary data 81.0–89.6%) and primary sensory area PB (weighted data 31.0–47.8%; binary data 16.9–20.1%) clustered less strongly than for the other parameter conditions. Referring to the orbito-temporo-insular cluster, both cases indicated a tendency to split into an orbito-insular and a temporal subgroup. For the weighted data, the association between these two groups was even low enough to fall below the cluster threshold (46.1%). Temporal areas TG, TH and A associated by 98.9–100% (binary data) and 100% (weighted data), respectively. Orbitofrontal area 13 and anterior insular area IA also showed an association of 100% for both classifications, whereas the frontal opercular area FCop had a somewhat lower association (weighted data 57.5%; binary data 93.9%). Like the two former clusters, the visual cluster also remains remarkably stable for both data classifications: areas OA, OB, OC, TA and TE still associate by 98.4–99.7% (weighted data) and 96.5–99.7% (binary data). Area TEO remains less strongly connected, (weighted data 46.1%; binary data 76.3%), whereas area TF prefers a rather loose association with posterior cingulate area LC (weighted data 56.1%; binary data 66.6%).

(d) *Statistical analysis of the optimal set analysis results*

Statistical analysis of OSA results showed a very low correlation between the results of any random data set and the real data. Absolute values of the correlation coefficients ranged between $r = 0.0005$ and $r = 0.0784$ (mean = 0.0236; s.d. = 0.0193), thus clearly demonstrating that the clusters computed by OSA from the real data were extremely unlikely to have been obtained by chance.

The analyses of the minimum costs for optimal solutions across all data sets were highly compatible. The distribution of minimum costs for optimal solutions from all 20 random data sets was characterized by a mean of 166.5 and a standard deviation of 3.8182. The minimum cost for optimal solutions for the original data, however, was more than nine standard deviations lower, that is 132. Compared to the distribution for random data, this shows that it is extremely unlikely that any random network has a structure with similarly low numbers of violations against the cluster rules as the real data.

By contrast, correlation between the OSA results for the original binary and weighted data was very high: for the balanced condition the correlation was $r = 0.82$, for high repulsion $r = 0.93$ and for the averaged condition $r = 0.83$. This also confirmed that the effects of different activity gradings for the original data were small.

(e) *Non-metric multidimensional scaling*

The results of the NMDS analyses were fully compatible with the cluster configurations obtained by OSA. Two-dimensional plots of NMDS representations of the interacting areas (figure 6*a*,*b* shows two typical examples) not only reproduced the three main clusters of the OSA solutions, but also gave further information about the overall structure of the network and the position of individual areas within it. For example, these plots confirmed well-established notions about the role of parietal areas, which had been less visible in the OSA solutions. Thus, they showed that the parietal areas have close affiliations to both somatomotor and visual areas, anterior parietal areas (PEm and PF) being more strongly orientated towards the somatomotor cluster and posterior parietal areas (PEp and PG) with a tendency to draw nearer the visual areas. Also, the intermediate position of prefrontal area 46 between motor and visual areas was emphasized. As for the visual areas, the unique position of the primary visual cortex (area OC) was demonstrated. Most interesting, however, was a clearly visible grouping of the visual areas into two lines, both of which originated from the primary visual cortex and were easily identified as parietal (PG, PEp, PF, PEm) and temporal visual areas (TEO, TE, TA, TF), respectively. For both of these streams, even the posterior–anterior topological sequence of the areas was reproduced fairly well. The NMDS plots also clearly showed the isolated position of sparsely interacting auditory area TC due to its exclusive interactions with the temporal areas TE and TA. As for the orbito-temporo-insular cluster, its subdivision into orbito-insular and temporal components which had been suggested by the high repulsion OSA solutions was confirmed by the NMDS analysis. Specifically, the NMDS results were compatible with the indications of OSA cluster plots about the higher cohesion of the temporal subgroup and the position of frontal opercular area FCop as the least strongly associated area within this cluster. Finally, the NMDS plots indicated that the primary sensory cortex (area PC) tended to take a unique position within the somatomotor system.

4. DISCUSSION

In the following, we discuss the main findings of this study, starting with the results of the graph theoretical 'small-world' analysis. The 'small-world' phenomenon has recently been described by Watts & Strogatz (1998), who introduced this term for a class of networks which combine a highly clustered structure with short average path length (i.e. high efficiency of communication). Such networks exhibit considerable advantages over both neighbourhood- and randomly connected networks, including enhanced signal–propagation speed, computational power and synchronizability with a minimal number of connections. Watts & Strogatz demonstrated that 'small-world' principles are found in complex social and biological systems, such as the nervous system of the nematode *Caenorhabditis elegans*. Suspecting that '...the small-world phenomenon is... probably generic for many large, sparse networks found in nature', they explicitly put forward the hypothesis that the primate brain also shows small-world architecture. To our knowledge, our study is the first investigation to support this hypothesis for functional interactions in the primate brain, while Hilgetag, Burns, O'Neill, Scannell & Young (this issue) demonstrate similar features of the structural organization of this system.

Whereas the fact of a clustered organization of the cortical network was apparent in the 'small-world' analysis, its actual configuration was revealed by the results of OSA and NMDS analyses. Application to differently classified (binary versus weighted) and differently mapped (hybrid map versus parcellation of

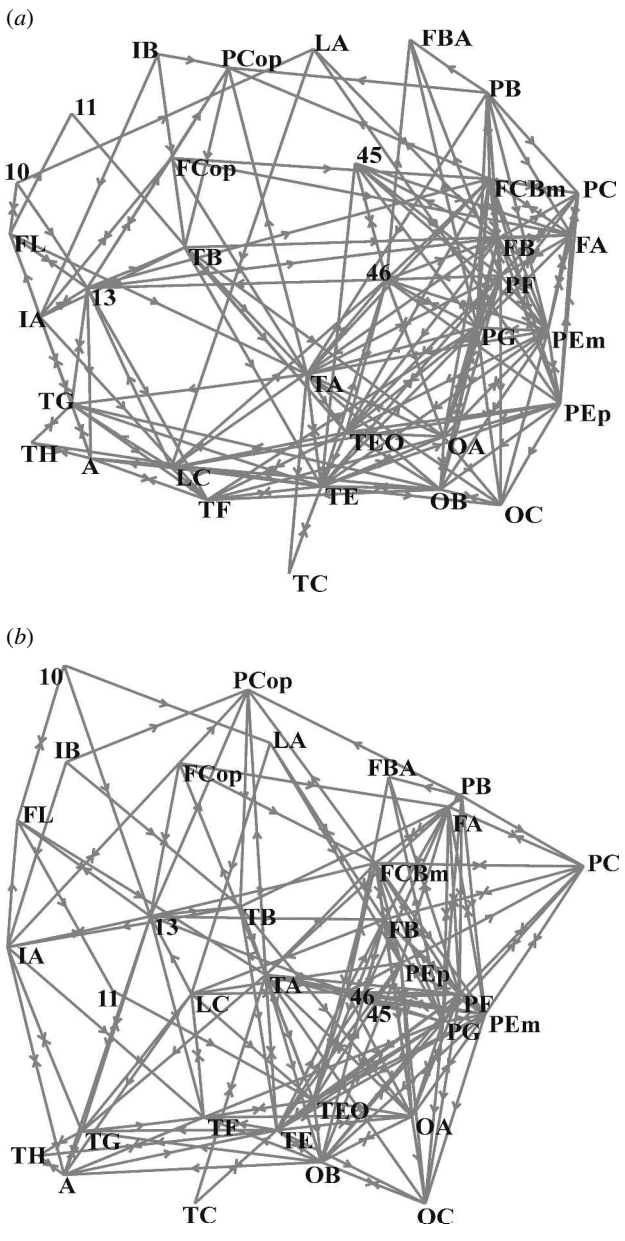

Figure 6. Two typical two-dimensional plots of a metric representation of the areal interactions in the network as obtained by NMDS. Generally, distances between areas are an inverse measure for the degree of similarity of their connectivity patterns (see § 2). Arrows between areas represent direction of observed activity spread. Areas 8A, 8B, 9 and 12, for which only absent interactions were reported (see table 1), were not included in this analysis. (*a*) Result from a two-dimensional NMDS analysis with a FIT value set to 1 (so-called 'STRESS'), under tied conditions. (*b*) Result from a two-dimensional NMDS analysis with a FIT value set to 2 (so-called 'SSTRESS'), under tied conditions (see Young *et al.* (1995) for details).

McCulloch) functional connectivity data delivered remarkably robust results (figure 7 summarizes the main findings of the OSA results). Are the resulting cluster configurations functionally plausible and compatible with what is already known about the functional organization of primate cerebral cortex?

Dealing with the somatomotor cluster first, the inseparability of precentral motor and postcentral somatosensory areas is not very surprising. The notion of their close integration has been suggested by findings on strong anatomical connections between primate primary motor and primary sensory areas (e.g. Stepniewska *et al.* 1993), and by analyses of the whole primate system of cortico-cortical connections (Young 1993; Young *et al.* 1994). It has also been confirmed repeatedly by functional studies. For example, lesion studies in monkeys demonstrated the necessity for somatosensory input to motor cortex for the acquisition of novel motor skills (Pavlides *et al.* 1993), and imaging experiments in humans showed that precentral and postcentral areas are not only jointly involved in actual motor performance but may also cooperate in motor imagery (Porro *et al.* 1996).

Evidence for the close participation of parietal areas in motor and sensory function has also been gained in recent years. This evidence concerned all lateral parts of parietal cortex (i.e. areas PEm, PG, PF and lateral portions of PEp in Von Bonin & Bailey's map). For example, recent single-neuron recordings in behaving monkeys demonstrated that the activity patterns of cells from posterior parietal areas LIP and PRR reflected changes of specific motor plans (Snyder *et al.* 1998). Reviewing experiments of single-unit recordings in superior parietal cortex of the macaque, Seal (1989) suggested that superior parietal cortex '. . . may function in the transformation of sensory activity into motor activity'. As for the integration of prefrontal area 46 into the somatomotor cluster, several anatomical tracer studies have demonstrated that area 46 is reciprocally connected with premotor and parietal areas (Barbas & Pandya 1987; Bates & Goldman-Rakic 1993; Cavada & Goldman-Rakic 1989; McGuire *et al.* 1991; Petrides & Pandya 1984). The NMDS analyses pointed to some additional relationships of parietal cortex and area 46 (figure 6*a*,*b*). For example, they showed the close relationships between posterior parietal (PEp, PG) and prestriate areas (OA, OB) whose cooperation in visuospatial functions is well established experimentally (Baizer *et al.* 1991; Colby *et al.* 1988; Ungerleider *et al.* 1998). Area 46 was assigned an intermediate position between motor and visual areas, thus reflecting its strong anatomical connections both with motor (see above) and visual areas (Barbas 1988; Schwartz & Goldman-Rakic 1984).

Turning to the visual cluster, some results of our analyses merit special attention. For both data classifications, high repulsion OSA led to the formation of distinct visual subclusters (figure 4*a*,*b*): prestriate areas OA and OB form a first, inferotemporal cortex TE and superior temporal cortex TA a second, and areas TF and TEO a third group. Striate cortex OC, although loosely associated to the second group, seems to take an independent position in this configuration. This configuration is clearly confirmed by the two-dimensional NMDS plots (figure 6*a*,*b*). Additionally, the latter clearly show a subdivision of the visual areas into the ventral and dorsal streams suggested by Ungerleider & Mishkin (1982). This suggested organization of the visual system has been given support both experimentally (see Ungerleider *et al.* 1998 for a summary) and by analyses of the visual system's anatomical connectivity (Young 1992; Young *et al.* 1994, 1995). Our global analysis of activation data delivers further evidence for this hypothesis. Startlingly, the data

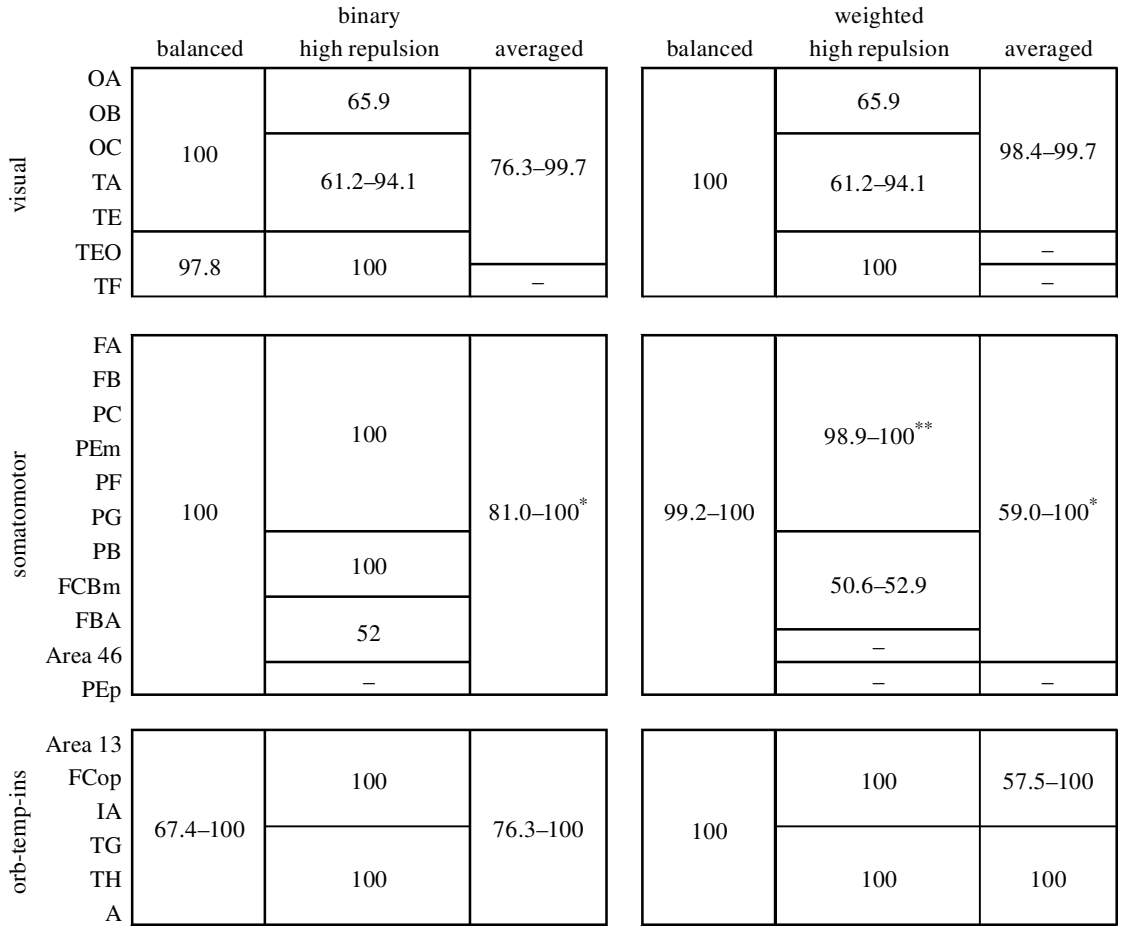

Figure 7. A summary of the OSA results across the different parameter constellations. A single asterisk designates two cases for which area PB was not included in the somatomotor cluster. In the case marked by a double asterisk, area FB showed an association of 51.8–52.9%. Values denote ranges of inter-areal associations (%) within the cluster (see figures 3, 4*b* and 5*a*).

on which our analysis is based were recorded with a rather crude technique more than 40 years ago. Appropriate analysis of them could therefore have anticipated by decades the first description of this important feature of the visual system's organization.

Interpretation of the orbito-temporo-insular cluster is less straightforward than the two previous cases. Anatomically, numerous tracing studies have shown that the areas of this cluster form a dense network of reciprocal connections (Carmichael & Price 1996; Mesulam & Mufson 1982*b*; Moran *et al.* 1987; Morecraft *et al.* 1992; Mufson & Mesulam 1982). Thus, the strong mutual interactions of these areas, which are expressed by their consistent clustering in OSA results, have well-documented anatomical counterparts. Functionally, the situation is less clear. Some authors have hypothesized that orbitofrontal and insular regions jointly form the cortical centre of gustatory information processing (Rolls 1989; Yaxley *et al.* 1990). Other proposals have grouped these areas together in the concept of the 'limbic system'. Pribram & MacLean (1953) and Mesulam & Mufson (1982*a*,*b*), for example, consider insula, lateral orbital surface and temporal pole as 'paralimbic areas with an olfactory allocortical focus'. Lately, the concept or concepts of the 'limbic system' have received an increasing amount of criticism on empirical and epistemological grounds (Blessing 1997; Kötter & Meyer 1992; Kötter & Stephan 1997; LeDoux 1991), and it has been argued that the assignment of the term 'limbic' to these areas has neither structural nor functional explanatory power. Nevertheless, the anatomically defined concept of Mesulam & Mufson (1982*b*) matches our functionally defined orbito-temporo-insular cluster surprisingly well: '...common connectivity patterns support the conclusion, based on architectonic observations, that the insulo-orbito-temporopolar component of the paralimbic brain should be considered as an integrated unit of cerebral organization'.

Having discussed experimental anatomical and physiological evidence for the cluster configurations revealed by OSA and NMDS analyses, we now address the general question of functional interpretations based on neuronographic data: does the method of strychnine neuronography give valid information about organizational principles of cerebral cortex, or do neuronographic data rather represent spread of unphysiological, and so uninteresting, hyperexcitation? This issue bears two aspects: the initial stimulus, the pharmacologically induced cortical disinhibition does not induce normal functional brain states, but leads to epileptiform activity in the areas involved. For this reason, strychnine and other pharmacological blockers of inhibition (such as penicilline and bicuculline) are standard models in epilepsy research (for recent examples see Holmes 1994; Kehne *et al.* 1997; Rostock *et al.* 1997). It is clear, however, that activity

propagation—be it physiologically normal or not—is constrained by the underlying anatomy. Therefore, organizational principles of cerebral cortex should be revealed by the activity patterns of both physiological and pathophysiological stimulation, the latter may even bring out these principles more clearly. This argument is supported by the findings of Hilgetag, Burns, O'Neill, Scannell & Young (this issue). The structural clusters that they computed from anatomical data on association fibre connectivity by means of OSA and NMDS bear a remarkably close relationship to the functional clusters revealed by this study: somatomotor, visual and orbitotemporo-insular groups are constitutive of the structural network as well. A statistical comparison of the cluster configurations for structural and functional connectivity has been prevented so far by the difficulty of translating between the different parcellation schemes underlying the two kinds of data (see below).

What is the contribution of this analysis to our understanding of the organizational principles of cerebral cortex? Advances in functional imaging techniques have generated a strong interest in analytical methods to aid the interpretation of functional data in terms of underlying anatomy, and especially with respect to the interactions between brain areas. A well-known example of this kind is the work of McIntosh and colleagues who have introduced the statistical technique of Structural Equation Modelling (SEM) to analyse data on functional interactions between cortical areas taking into account the constraints of known anatomical connectivity (McIntosh & Gonzalez-Lima 1991). SEM aims at determining 'path coefficients' within a given anatomically defined network (i.e. the functional impact one brain structure exerts on another via a given pathway). This method has been applied to characterize cortical networks in various functional contexts, for example object and spatial vision (McIntosh *et al.* 1994), working memory (McIntosh *et al.* 1996), attention to visual motion (Büchel & Friston 1997) and episodic memory retrieval (Kohler *et al.* 1998). Another recent approach by Tononi *et al.* (1998) is conceptually closely related to the principles of OSA. Within this approach, a 'functional cluster' is defined as a set of brain regions which interact more strongly among themselves than with the rest of the brain (see also Young *et al.* 1995). Tononi *et al.* (1998) extracted such functional clusters from imaging data by computing 'cluster indices' that indicate the degree of internal cohesion and external isolation of a given set of brain regions.

Compared to analyses on structural data (Burns & Young, this issue; Felleman & Van Essen 1991; Hilgetag *et al.* 1996; Jouve *et al.* 1997; Scannell *et al.* 1995; Young 1992, 1993), all available analytical studies on functional data have a considerable drawback: none has made use of a systematically collated database comprising a large number of individual experiments from different parts of the cortex. Only in this way, however, it is possible to aim at insights into global characteristics of cortical organization. Although initial databases of imaging data are currently being constructed (e.g. Roland & Zilles 1996), their use for analyses based on more than one study is hampered by the context-dependency of imaging (and other behaviour-related) experiments. Even minor differences in the underlying experimental paradigm can lead to considerably different sets of brain structures to become involved (see McIntosh *et al.* (1996) for an example where slight changes in recall time led to the activation of different cortical networks). Due to this context dependency, such experiments are difficult to compare, thus restricting analytical approaches to the results of a single study. At best, the existing databases on functional data may help to clarify the role of a specific brain structure in different functional contexts (e.g. Paus *et al.* 1998).

Context dependency, however, is not a significant problem for strychnine neuronography. Activity patterns resulting from local strychnine application have been described to be reproducible within the same animal and stable for a given area across animals (Dusser de Barenne & McCulloch 1938). This high context independence of the induced activity patterns is explicable by the intracortical mode of stimulation and the high strength of the applied stimulus. Blocking cortical inhibition with high-potency strychnine is a very strong stimulus sufficient to ensure that the locally induced overexcitation is propagated via the association fibres of the affected cortex, irrespective of the functional state of the remaining cortex (Chatt & Ebersole 1988; Klee *et al.* 1992). Context independence of strychnine-induced activity patterns may be further enhanced by the use of barbiturates and ether for anaesthesia under which the animals were kept (see neuronography references above). Although studies on the impact of anaesthesia on cortical activity have delivered complex and partially contradictory results, it seems likely that by different mechanisms anaesthetics generally lead to a decrease of excitatory and to an increase of inhibitory activity (El-Beheiry & Puil 1989; Pocock & Richards 1993). It is especially well established for barbiturates that they diminish release of excitatory transmitters, enhance inhibitory synaptic transmission and increase affinity of $GABA_A$ to its receptor (Pocock & Richards 1993). Furthermore, Bowery & Dray (1976) showed that the disinhibitory effects of locally applied strychnine can be reduced by barbiturates. Finally, there is some evidence that most anaesthetics, including barbiturates and ether, primarily impair thalamocortical functional connectivity (and thus the influence of sensory stimuli) but have comparatively small effects on cortical activity as such (Angel 1991, 1993). These findings together suggest for strychnine neuronography that (i) evoked activity patterns are not strongly altered by anaesthetics; and (ii) local overexcitation due to strychnine application is achieved even in spite of enhanced inhibitory mechanisms.

It should be pointed out, however, that strychnine neuronography does not seem to be an appropriate method for all parts of the nervous system. For example, it was found that strychnine failed to elicit any activity in the cerebellum, the olfactory bulb and the vagal nucleus (Dow 1938; Frankenhaeuser 1951). This is probably due to the fact that initiation, sustenance and propagation of the local disinhibition by the action of strychnine on $GABA_A$ and glycine receptors depends on both the respective receptor distributions and the microcircuitry of the strychninized region. Apparently, in spite of regional differences in microcircuitry and distributions of glycine (Fujita *et al.* 1991; Naas *et al.* 1991; Sato *et al.* 1992) and

$GABA_A$ receptors (Gebhard *et al.* 1995; Geyer *et al.* 1998; Kritzer *et al.* 1992), the cerebral cortex generally seems to be more susceptible to strychnine than other parts of the brain. This constraint has certainly contributed to the fact that since the mid-1950s strychnine neuronography has lost its former importance for the characterization of functional interactions and has successively been replaced by methods of electrical stimulation. Also, it aggravates comparisons between the strength of elicited responses from different cortical regions. In this study, we took this uncertainty into account by performing the analyses both for weighted and binary data (see above).

On the whole, this study is the first attempt to unravel context-independent global characteristics of functional organization of cerebral cortex on the basis of a database containing results from a large number of experiments. It shows that modern computational analysis of neuronographic data provides a global view on the organizational principles of primate cerebral cortex that is compatible with the overall picture from modern experimental investigations. Surprisingly, a single, albeit large, collection of context-insensitive functional data is sufficient to account for many insights gained by a multitude of context-sensitive experimental approaches. In spite of their age and their methodological restrictions, neuronographic experiments still represent a unique source of systematic data on functional connectivity of cerebral cortex. Their quality is indirectly confirmed by the results of our analyses. The global network defined by neuronographic data shows properties that could not have been produced by random data, and its structure is compatible with recent studies, including very detailed features, such as the differentiation of the visual system into ventral and dorsal streams of processing. The most important global properties of this functional network of primate cerebral cortex are as follows.

(i) Three independent methods of analysis ('small-world' analysis, OSA, NMDS) showed that the functional network of interactions within cerebral cortex is not homogeneous, but is characterized by a highly clustered structure.

(ii) Graph-theoretical analysis revealed that the cortical network is likely to be a 'small-world' network. This is empirical evidence for the recent hypothesis of Watts & Strogatz (1998), see above.

(iii) OSA and NMDS results showed that cortical areas form three main groups with high intrinsic and low extrinsic functional interactions: a somatomotor cluster, a visual cluster and an orbito-insular-temporal cluster. These results were remarkably robust across the different classifications and mappings of the data (figure 7) and are compatible with a variety of experimental findings.

As mentioned above, Hilgetag, Burns, O'Neill, Scannell & Young (this issue) performed identical analyses on anatomical connectivity data, with results compatible with ours. Due to the different parcellation schemes, however, a statistical quantification of the similarity of cluster configurations for structural and functional connectivity has been prevented so far. However, this is becoming possible by means of recently developed databases containing structural connectivity and areal relationships between the different parcellation schemes involved, so that Objective Relational Transformation (ORT; see the companion paper of Stephan *et al.*, this issue) can be used to map the data into a common descriptive space. Statistical analysis of structurally and functionally defined clusters is thus being made possible, and the detailed nature of the structure–function relationships indicated by Hilgetag, Burns, O'Neill, Scannell & Young (this issue) and this paper will be specified in more detail in the future.

We thank Jack W. Scannell and Axel Schleicher for their helpful advice on the statistical evaluation, and Christine Opfermann-Rüngeler for help with figure 1. This work was made possible by a Wellcome Trust Collaboration Grant to M.P.Y. and R.K. C.C.H. is supported by a Wellcome Prize Scholarship and K.E.S. by the German National Merit Foundation (Studienstiftung des Dt. Volkes) and the Neuroscientific Graduate School of Düsseldorf University (Graduiertenkolleg 'Pathologische Prozesse des Nervensystems').

REFERENCES

Angel, A. 1991 The G.L. Brown lecture. Adventures in anaesthesia. *Exp. Physiol.* **76,** 1–38.

Angel, A. 1993 Central neuronal pathways and the process of anaesthesia. *Br. J. Anaesth.* **71**, 148–163.

Bailey, P., Von Bonin, G., Davis, E. W., Garol, H. W., McCulloch, W. S., Roseman, E. & Silveira, A. 1944*a* Functional organization of the medial aspect of the cortex. *J. Neurophysiol.* **7**, 51–55.

Bailey, P., Von Bonin, G., Davis, E. W., Garol, H. W. & McCulloch, W. S. 1944*b* Further observations on associational pathways in the brain of *Macaca mulatta*. *J. Neuropath. Exp. Neurol.* **3**, 413–415.

Bailey, P., Von Bonin, G., Garol, H. W. & McCulloch, W. S. 1943*a* Functional organization of temporal lobe of monkey (*Macaca mulatta*) and chimpanzee (*Pan satyrus*). *J. Neurophysiol.* **6**, 121–128.

Bailey, P., Von Bonin, G., Garol, H. W. & McCulloch, W. S. 1943*b* Long association fibres in the cerebral hemispheres of monkey and chimpanzee. *J. Neurophysiol.* **6,** 129–134.

Baizer, J. S., Ungerleider, L. G. & Desimone, R. 1991 Organization of visual inputs to the inferior temporal and posterior parietal cortex in macaques. *J. Neurosci.* **11**, 168–190.

Barbas, H. 1988 Anatomic organization of basoventral and mediodorsal visual recipient prefrontal regions in the rhesus monkey. *J. Comp. Neurol.* **276**, 313–342.

Barbas, H. & Pandya, D. N. 1987 Architecture and frontal cortical connections of the premotor cortex (area 6) in the rhesus monkey. *J. Comp. Neurol.* **256**, 211–228.

Barbas, H. & Pandya, D. N. 1989 Architecture and intrinsic connections of the prefrontal cortex in the rhesus monkey. *J. Comp. Neurol.* **286**, 353–375.

Bates, J. F. & Goldman-Rakic, P. S. 1993 Prefrontal connections of medial motor areas in the rhesus monkey. *J. Comp. Neurol.* **336**, 211–228.

Blessing, W. W. 1997 Inadequate frameworks for understanding bodily homeostasis. *Trends Neurosci.* **20**, 235–239.

Bowery, N. G. & Dray, A. 1976 Barbiturate reversal of amino acid antagonism produced by convulsant agents. *Nature* **264**, 276–278.

Büchel, C. & Friston, K. J. 1997 Modulation of connectivity in visual pathways by attention: cortical interactions evaluated with structural equation modelling and fMRI. *Cerebr. Cortex* **7**, 768–778.

Burns, G. A. P. C. 1997 Neural connectivity of the rat: theory, methods and applications. DPhil thesis, University of Oxford, UK.

Carmichael, S. T. & Price, J. L. 1994 Architectonic subdivision of the orbital and medial prefrontal cortex in the macaque monkey. *J. Comp. Neurol.* 346, 366–402.

Carmichael, S. T. & Price, J. L. 1996 Connectional networks within the orbital and medial prefrontal cortex of macaque monkeys. *J. Comp. Neurol.* **371**, 179–207.

Cavada, C. & Goldman-Rakic, P. S. 1989 Posterior parietal cortex in rhesus monkey: II. Evidence for segregated cortico-cortical networks linking sensory and limbic areas with the frontal lobe. *J. Comp. Neurol.* **287**, 422–445.

Chatt, A. B. & Ebersole, J. S. 1988 Comparisons between strychnine and penicillin epileptogenesis suggest that propagating epileptiform abnormalities require the potentiation of thalamocortical circuitry in neocortical layer 4. *Exp. Neurol.* **100**, 365–380.

Chusid, J. G., Sugar, O. & French, J. D. 1948 Corticocortical connections of the cerebral cortex lying within the arcuate and lunate sulci of the monkey (*Macaca mulatta*). *J. Neuropath. Exp. Neurol.* **7**, 439–446.

Colby, C. L., Gattass, R., Olson, C. R. & Gross, C. G. 1988 Topographical organization of cortical afferents to extrastriate visual area PO in the macaque: a dual tracer study. *J. Comp. Neurol.* **269**, 392–413.

Dow, R. S. 1938 The electrical activity of the cerebellum and its functional significance. *J. Physiol.* **94**, 67–86.

Dusser de Barenne, J. G. 1924 Experimental researches on sensory localization in the cerebral cortex of the monkey (*Macacus*). *Proc. R. Soc. Lond.* B **96**, 272–291.

Dusser de Barenne, J. G. & McCulloch, W. S. 1938 Functional organization in the sensory cortex of the monkey (*Macaca mulatta*). *J. Neurophysiol.* **1**, 69–85.

Dusser de Barenne, J. G. & McCulloch, W. S. 1939 Physiological delimitation of neurones in the central nervous system. *Am. J. Neurophysiol.* **127**, 621–628.

Dusser de Barenne, J. G., McCulloch, W. S. & Ogawa, T. 1938 Functional organization in the face-subdivision of the sensory cortex of the monkey (*Macaca mulatta*). *J. Neurophysiol.* **1**, 436–441.

Dusser de Barenne, J. G., Garol, H. W. & McCulloch, W. S. 1941 Functional organization of sensory and adjacent cortex of the monkey. *J. Neurophysiol.* **4**, 324–330.

Dunsmore, R. H. & Lennox, M. A. 1950 Stimulation and strychninization of supracallosal anterior cingulate cortex. *J. Neurophysiol.* **13**, 207–214.

El-Beheiry, H. & Puil, E. 1989 Anaesthetic depression of excitatory synaptic transmission in neocortex. *Exp. Brain Res.* **77**, 87–93.

Felleman, D. J. & Van Essen, D. C. 1991 Distributed hierarchical processing in the primate cerebral cortex. *Cerebr. Cortex* **1**, 1–47.

Frankenhaeuser, B. 1951 Limitations of method of strychnine neuronography. *J. Neurophysiol.* **14**, 73–79.

French, J. D., Sugar, O. & Chusid, J. G. 1948 Corticocortical connections of the superior bank of the sylvian fissure in the monkey (*Macaca mulatta*). *J. Neurophysiol.* **11**, 185–192.

Friston, K. J. 1994 Functional and effective connectivity in neuroimaging: a synthesis. *Hum. Brain Mapp.* **2**, 56–78.

Fujita, M., Sato, K., Sato, M., Inoue, T., Kozuka, T. & Tohyama, M. 1991 Regional distribution of the cells expressing glycine receptor b subunit mRNA in the rat brain. *Brain Res.* **460**, 23–37.

Gebhard, R., Zilles, K., Schleicher, A., Everitt, B. J., Robbins, T. W. & Divac, I. 1995 Parcellation of the frontal cortex of the New World monkey *Callithrix jacchus* by eight neurotransmitter-binding sites. *Anat. Embryol.* (*Berl.*) **191**, 509–517.

Geyer, S., Matelli, M., Luppino, G., Schleicher, A., Jansen, Y., Palomero-Gallagher, N. & Zilles, K. 1998 Receptor autoradiographic mapping of the mesial motor and premotor cortex of the macaque monkey. *J. Comp. Neurol.* **397**, 231–250.

Hilgetag, C. C., O'Neill, M. A. & Young, M. P. 1996 Indeterminate organization of the visual system. *Science* **271**, 776–777.

Hilgetag, C. C., Stephan, K. E., Burns, G. A. P. C., O'Neill, M. A., Young, M. P., Zilles, K. & Kötter, R. 1997 Systems of primate cortical areas defined by functional connectivity. *Soc. Neurosci. Abstr.* **23**, 514.13.

Hilgetag, C. C., Burns, G. A. P. C., O'Neill, M. A. & Young, M. P. 1998 Cluster structure of cortical systems in mammalian brains. In *Computational neuroscience: trends in research*, (ed. J. M. Bower), pp. 41–46. New York, London: Plenum Press.

Holmes, O. 1994 The intracortical neuronal connectivity subserving focal epileptiform activity in rat neocortex. *Exp. Physiol.* **79**, 705–721.

Jouve, B., Rosenstiehl, P. & Imbert, M. 1998 A mathematical approach to the connectivity between the cortical visual areas of the macaque monkey. *Cerebr. Cortex.* **8**, 28–39.

Kehne, J. H., Kane, J. M., Chaney, S. F., Hurst, G., McCloskey, T. C., Petty, M. A., Senyah, Y., Wolf, H. H., Zobrist, R. & White, H. S. 1997 Preclinical characterization of MDL 27,192 as a potential broad spectrum anticonvulsant agent with neuroprotective properties. *Epilepsy Res.* **27**, 41–54.

Klee M. R., Shirasaki, T., Nakaye, T., Akaike, N. & Melikov, E. N. 1992 Interaction of strychnine and bicuculline with GABA- and glycine-induced chloride currents in isolated CA1 neurons. In *Epilepsy and inhibition* (ed. E. J. Speckmann & M. J. Gutnick), pp. 93–106. Munich, Germany: Urban & Schwarzenberg.

Kohler, S., McIntosh, A. R., Moscovitch, M. & Winocur, G. 1998 Functional interactions between the medial temporal lobes and posterior neocortex related to episodic memory retrieval. *Cerebr. Cortex* **8**, 451–461.

Kötter, R. & Meyer, N. 1992 The limbic system: a review of its empirical foundation. *Behav. Brain Res.* **52**, 105–127.

Kötter, R. & Stephan, K. E. 1997 Useless or helpful? The 'limbic system' concept. *Rev. Neurosci.* **8**, 139–146.

Kritzer, M. F., Cowey, A. & Somogyi, P. 1992 Patterns of inter- and intralaminar GABAergic connections distinguish striate (V1) and extrastriate (V2, V4) visual cortices and their functionally specialized subdivisions in the rhesus monkey. *J. Neurosci.* **12**, 4545–4564.

LeDoux, J. E. 1991 Emotion and the limbic system concept. *Concepts Neurosci.* **2**, 169–199.

McCulloch, W. S. 1944 The functional organization of the cerebral cortex. *Physiol. Rev.* **24**, 390–407.

McGuire, P. K., Bates, J. F. & Goldman-Rakic, P. S. 1991 Interhemispheric integration. I. Symmetry and convergence of the corticocortical connections of the left and the right principal sulcus (PS) and the left and the right supplementary motor area (SMA) in the rhesus monkey. *Cerebr. Cortex* **1**, 390–407.

McIntosh, A. R. & Gonzalez-Lima, F. 1991 Structural modeling of functional neural pathways mapped with 2-deoxyglucose: effects of acoustic startle habituation on the auditory system. *Brain Res.* **547**, 295–302.

McIntosh, A. R., Grady, C. L., Ungerleider, L. G., Haxby, J. V., Rapoport, S. I. & Horwitz, B. 1994 Network analysis of cortical visual pathways mapped with PET. *J. Neurosci.* **14**, 655–666.

McIntosh, A. R., Grady, C. L., Haxby, J. V., Ungerleider, L. G. & Horwitz, B. 1996 Changes in limbic and prefrontal functional interactions in a working memory task for faces. *Cerebr. Cortex* **6**, 571–584.

Mesulam, M. M. & Mufson, E. J. 1982*a* Insula of the old world monkey. I. Architectonics in the insulo-orbito-temporal component of the paralimbic brain. *J. Comp. Neurol.* **212**, 1–22.

Mesulam, M. M. & Mufson, E. J. 1982*b* Insula of the old world monkey. III. Efferent cortical output and comments on function. *J. Comp. Neurol.* 1982 **212**, 38–52.

Moran, M. A., Mufson, E. J. & Mesulam, M. M. 1987 Neural inputs to the temporopolar cortex of the rhesus monkey. *J. Comp. Neurol.* **256**, 88–103.

Morecraft, R. J., Geula, C. & Mesulam, M. M. 1992 Cytoarchitecture and neural afferents of orbitofrontal cortex in the brain of the monkey. *J. Comp. Neurol.* **323**, 341–358.

Mufson, E. J. & Mesulam, M. M. 1982 Insula of the old world monkey. II. Afferent cortical input and comments on the claustrum. *J. Comp. Neurol.* **212**, 23–37.

Naas, E., Zilles, K., Gnahn, H., Betz, H., Becker, C. M. & Schröder, H. 1991 Glycine receptor immunoreactivity in rat and human cerebral cortex. *Brain Res.* **561**, 139–146.

Pandya, D. N. & Seltzer, B. 1982 Intrinsic connections and architectonics of posterior parietal cortex in the rhesus monkey. *J. Comp. Neurol.* **204**, 196–210.

Paus, T., Koski, L., Caramanos, Z. & Westbury, C. 1998 Regional differences in the effects of task difficulty and motor output on blood flow response in the human anterior cingulate cortex: a review of 107 PET activation studies. *NeuroReport* **9**, 37–47.

Pavlides, C., Miyashita, E. & Asanuma, H. 1993 Projection from the sensory to the motor cortex is important in learning motor skills in the monkey. *J. Neurophysiol.* **70**, 733–741.

Petr, R., Holden, L. B. & Jirout, J. 1949 The efferent intercortical connections of the superficial cortex of the temporal lobe (*Macaca mulatta*). *J. Neuropath. Exp. Neurol.* **8**, 100–103.

Petrides, M. & Pandya, D. N. 1984 Projections to the frontal cortex from the posterior parietal region in the rhesus monkey. *J. Comp. Neurol.* **228**, 105–116.

Preuss, T. M. & Goldman-Rakic, P. S. 1991 Myelo- and cytoarchitecture of the granular frontal cortex and surrounding regions in the strepsirhine primate Galago and the anthropoid primate Macaca. *J. Comp. Neurol.* **310**, 429–474.

Pribram, K. H., Lennox, M. A. & Dunsmore, R. H. 1950 Some connections of the orbito-fronto-temporal, limbic and hippocampal areas of *Macaca mulatta*. *J. Neurophysiol.* **13**, 127–135.

Pribram, K. H. & MacLean, P. D. 1953 Neuronographic analysis of medial and basal cerebral cortex comparing monkey and cat. II. Monkey. *J. Neurophysiol.* **16**, 324–340.

Pocock, G. & Richards, C. D. 1993 Excitatory and inhibitory synaptic mechanisms in anaesthesia. *Br. J. Anaesth.* **71**, 134–147.

Porro, C. A., Francescato, M. P., Cettolo, V., Diamond, M. E., Baraldi, P., Zuiani, C., Bazzocchi, M. & di Prampero, P. E. 1996 Primary motor and sensory cortex activation during motor performance and motor imagery: a functional magnetic resonance imaging study. *J. Neurosci.* **16**, 7688–7698.

Roland, P. E. & Zilles, K. 1996 The developing European computerized human brain database for all imaging modalities. *NeuroImage* **4**, 39–47.

Rolls, E. T. 1989 Information processing in the taste system of primates. *J. Exp. Biol.* **146**, 141–164.

Rostock, A., Tober, C., Rundfeldt, C., Bartsch, R., Unverferth, K., Engel, J., Wolf, H. H. & White, H. S. 1997 AWD 140-190: a new anticonvulsant with a very good margin of safety. *Epilepsy Res.* **28**, 17–28.

Sato, K., Kiyama, H. & Tohyama, M. 1992 Regional distribution of cells expressing glycine receptor alpha 2 subunit mRNA in the rat brain. *Brain Res.* **590**, 95–108.

Scannell, J. W., Blakemore, C. & Young, M. P. 1995 Analysis of connectivity in the cat cerebral cortex. *J. Neurosci.* **15**, 1463–1483.

Schwartz, M. L. & Goldman-Rakic, P. S. 1984 Callosal and intrahemispheric connectivity of the prefrontal association cortex in rhesus monkey: relation between intraparietal and principal sulcal cortex. *J. Comp. Neurol.* **226**, 403–420.

Seal, J. 1989 Sensory and motor functions of the superior parietal cortex of the monkey as revealed by single-neuron recordings. *Brain Behav. Evol.* **33**, 113–117.

Shirasaki, T., Klee, M. R., Nakaye, T. & Akaike, N. 1991 Differential blockade of bicuculline and strychnine on GABA- and glycine-induced responses in dissociated rat hippocampal pyramidal cells. *Brain Res.* **561**, 77–83.

Snyder, L. H., Batista, A. P. & Andersen, R. A. 1998 Change in motor plan, without a change in the spatial locus of attention, modulates activity in posterior parietal cortex. *J. Neurophysiol.* **79**, 2814–2819.

Sommer, F. & Kötter, R. 1997 Simulating a network of cortical areas using anatomical connection data in the cat. In *Computational neuroscience: trends in research* (ed. J. M. Bower), pp. 511–517. New York: Plenum.

Stepniewska, I., Preuss, T. M. & Kaas, J. H. 1993 Architectonics, somatotopic organization, and ipsilateral cortical connections of the primary motor area (M1) of owl monkeys. *J. Comp. Neurol.* **330**, 238–271.

Sugar, O., French, J. D. & Chusid, J. G. 1948 Corticocortical connections of the superior surface of the temporal operculum in the monkey. *J. Neurophysiol.* **11**, 175–184.

Sugar, O., Amador, L. V. & Griponissiotis, B. 1950*a* Corticocortical connections of posterior wall of central sulcus in monkey. *J. Neurophysiol.* **13**, 229–233.

Sugar, O., Amador, L. V. & Griponissiotis, B. 1950*b* Corticocortical connections of the walls of the superior temporal sulcus in the monkey (*Macaca mulatta*). *J. Neuropath. Exp. Neurol.* **9**, 179–185.

Sugar, O., Petr, R., Amador, L. V. & Griponissiotis, B. 1950*c* Corticocortical connections of the cortex buried in the intraparietal and principal sulci of the monkey (*Macaca mulatta*). *J. Neuropath. Exp. Neurol.* **9**, 430–437.

Takahashi, Y., Shirasaki, T., Yamanaka, H., Ishibashi, H. & Akaike, N. 1994 Physiological roles of glycine and gamma-aminobutyric acid in dissociated neurons of rat visual cortex. *Brain Res.* **640**, 229–235.

Tononi, G., McIntosh, A. R., Russell, D. P. & Edelman, G. M. 1998 Functional clustering: identifying strongly interactive brain regions in neuroimaging data. *NeuroImage* **7**, 133–149.

Ungerleider, L. G., Courtney, S. M. & Haxby, J. V. 1998 A neural system for human visual working memory. *Proc. Natl Acad. Sci. USA* **95**, 883–890.

Ungerleider, L. G. & Mishkin, M. 1982 Two cortical visual systems. In *Analysis of visual behavior* (ed. D. G. Ingle, M. A. Goodale & R. J. Q. Mansfield), pp. 549–586. Cambridge, MA: MIT Press.

Von Bonin, G. & Bailey, P. 1947 *The neocortex of* Macaca mulatta. Urbana, IL: University of Illinois Press.

Von Bonin, G., Garol, H. W. & McCulloch, W. S. 1942 The functional organization of the occipital lobe. *Biol. Symposia* **7**, 165–192.

Walker, E. A. 1940 A cytoarchitectural study of the prefrontal area of Macaque monkey. *J. Comp. Neurol.* **73**, 59–86.

Ward, A. A., Peden, J. K. & Sugar, O. 1946 Cortico-cortical connections in the monkey with special reference to area 6. *J. Neurophysiol.* **9**, 453–462.

Watts, D. J. & Strogatz, S. H. 1998 Collective dynamics of 'small-world' networks. *Nature* **393**, 440–442.

Yaxley, S., Rolls, E. T. & Sienkiewicz, Z. J. 1990 Gustatory responses of single neurons in the insula of the macaque monkey. *J. Neurophysiol.* **63**, 689–700.

Young, M. P. 1992 Objective analysis of the topological organization of the primate cortical visual system. *Nature* **358**, 152–155.

Young, M. P. 1993 The organization of neural systems in the primate cerebral cortex. *Proc. R. Soc. Lond.* B **252**, 13–18.

Young, M. P., Scannell, J. W. & Burns, G. A. P. C. 1994 *The analysis of cortical connectivity*. Heidelberg, Germany: Springer.

Young, M. P., Scannell, J. W., O'Neill, M. A., Hilgetag, C. C., Burns, G. & Blakemore, C. 1995 Non-metric multidimensional scaling in the analysis of neuroanatomical connection data and the organization of the primate cortical visual system. *Phil. Trans. R. Soc. Lond.* B **348**, 281–308.